Numerical Techniques to Solve Condensational and Dissolutional Growth Equations When Growth is Coupled to Reversible Reactions

Mark Z. Jacobson
DEPARTMENT OF CIVIL ENGINEERING, STANFORD UNIVERSITY, STANFORD, CALIFORNIA 94305-4020

ABSTRACT. Noniterative, unconditionally stable numerical techniques for solving condensational and dissolutional growth equations are given. Growth solutions are compared to Gear-code solutions for three cases when growth is coupled to reversible equilibrium chemistry. In all cases, results from the new growth schemes matched Gear-code solutions nearly exactly when growth and equilibrium calculations were operator-split with a 1 s time interval. Results also matched well for a 15 s interval. With a 15 s interval, the growth-equilibrium schemes can be used in a three-dimensional model. Longer operator splitting intervals, in some cases, induced oscillations in concentrations caused by delays in feedback between equilibrium and growth calculations. Simulation results indicated that gases and aerosols were closer to equilibrium when the relative humidity was 90% than when it was 40%. AEROSOL SCIENCE AND TECHNOLOGY 27:491–498 (1997) **© 1997 American Association for Aerosol Research**

INTRODUCTION

Among the processes affecting the size distribution and composition of atmospheric aerosols and cloud drops are condensation, dissolution, and evaporation. Several numerical methods have been developed to simulate condensation and evaporation. These include finite element methods (e.g., Varoglu and Finn, 1980; Tsang and Brock, 1986; Tsang and Huang, 1990), discrete size bin methods (e.g., Gelbard and Seinfeld, 1980; Toon et al., 1988; Rao and McMurry, 1989), the cubic spline method (e.g., Middleton and Brock, 1976), modified upwind difference methods (e.g., Smolarkiewicz, 1983; Tsang and Korgaonkar, 1987), and moments methods (e.g., Friedlander, 1983; Whitby, 1985; Lee, 1985; Brock et al., 1986). Dissolution and evaporation in dilute solutions have also been simulated in a number of papers (e.g., Schwartz, 1984; Chameides, 1984; Jacob, 1986; Pandis and Seinfeld, 1989; Bott and Carmichael, 1993; Sander et al., 1995). One paper proposed a model that simulates dissolution and evaporation in concentrated solutions (Wexler and Seinfeld, 1991).

Numerical studies of aerosols require that growth and chemistry equations be solved at high ionic strengths. Only the last paper listed above considered growth in aerosols at high ionic strengths, but results were not reported for three dimensions. Because aerosols affect spatial gas and radiative fields, their simulation in three-dimensions is important. In this paper, noniterative, unconditionally stable solutions to condensational and dissolutional growth equations

Aerosol Science and Technology 27:491–498 (1997)

Published by Elsevier Science Inc.

0278-6826/97/$17.00
PII S0278-6826(97)00107-4

are given. Both schemes are computationally fast; yet, to simulate aerosol growth at high ionic strengths, they must be coupled to an equilibrium solver, which is slower. The coupled growth/equilibrium model discussed is still fast enough to be used in three dimensions. Predictions from the model are compared to those from a coupled ordinary differential equation solver/equilibrium scheme for three cases.

GROWTH EQUATIONS

An equation describing condensational growth of a component q onto particles of size i and subsequent reversible reaction is

$$\frac{dc_{q,i}}{dt} = k_{q,i}(C_q - S'_{q,i}C_{q,s,i}) + \left(\frac{dc_{q,i}}{dt}\right)_{\text{eq}} \quad (1)$$

(Jacobson, 1997a), where $c_{q,i}$ is the mole concentration of species q in size bin i (moles cm^{-3} air), C_q is the ambient vapor mole concentration of species q in the gas phase (moles cm^{-3} air), $C_{q,s,i}$ is the surface vapor mole concentration of a condensing species over a flat surface (moles cm^{-3} air), $k_{q,i}$ is the mass transfer rate between the gas phase and all particles of size i (s^{-1}), $S'_{q,i}$ is the saturation ratio at equilibrium, and $(dc_{q,i,t}/dt)_{\text{eq}}$ is the rate of change in particle concentration of the species due to reversible equilibrium reactions (e.g., dissociation, precipitation, etc.).

The mass transfer rate in Eq. (1) can be approximated as $k_{q,i} = n_i 4\pi r_i D^{\text{eff}}_{q,i}$, where n_i is the number concentration of particles of size i (partic. cm^{-3}), r_i is the fluctuating radius of a single particle, and $D^{\text{eff}}_{q,i}$ is an effective diffusion coefficient (cm^2 s^{-1}) that accounts for the geometry of vapor collision with small particles and ventilation of heat and vapor during sedimentation of large particles containing liquid water. One expression for $D^{\text{eff}}_{q,i}$ is given in Jacobson and Turco (1995).

For condensational growth, $C_{q,s,i}$ is often parameterized empirically or calculated from the Clausius–Clapeyron equation. For dissolutional and surface reaction growth, $C_{q,s,i}$ is a function of particle composition. The surface vapor concentration of a soluble, nondissociating species over a dilute solution is

$$C_{q,s,i} = \frac{\mathbf{m}_{q,i}}{1000R^*TH_q} = \frac{c_{q,i}}{m_w c_{w,i} R^* T H_q} = \frac{c_{q,i}}{H'_{q,i}}, \quad (2)$$

where $\mathbf{m}_{q,i} = 1000c_{q,i}/m_w c_{w,i}$ is the molality of species q in solution (mole kg^{-1}), R^* is the ideal gas constant (L atm mole^{-1} K^{-1}), T is temperature (K), H_q is the Henry's constant of the species (moles kg^{-1} atm^{-1}), $c_{q,i}$ is the mole concentration of dissolved gas q in size bin i (moles cm^{-3}-air), $c_{w,i}$ is the mole concentration of liquid water in size bin i, m_w is the molecular weight of water (g mole^{-1}), and $H'_{q,i} = m_w c_{w,i} R^* T H_q$. Substituting Eq. (2) into Eq. (1) gives

$$\frac{dc_{q,i}}{dt} = k_{q,i}\left(C_q - S'_{q,i}\frac{c_{q,i}}{H'_{q,i}}\right) + \left(\frac{dc_{q,i}}{dt}\right)_{\text{eq}}, \quad (3)$$

which is the rate of change of $c_{q,i}$ due to dissolutional growth/evaporation.

When strong acids or bases dissolve in solution, they dissociate. Hydrochloric acid (HCl) and ammonia (NH_3) dissociate to H^+/Cl^- and NH_4^+/OH^-, respectively. In such cases, $H'_{q,i}$ in Eq. (3) can be replaced with

$$H'_{\text{CL}^-,i} = \frac{m_w c_{w,i} R^* T K_{\text{HCl}}}{\mathbf{m}_{H^+,i}\gamma^2_{i,\text{H}^+/\text{Cl}^-}}, \quad (4)$$

$$H'_{\text{NH}_4^+,i} = \frac{\mathbf{m}_{\text{H}^+,i}\gamma_{i,\text{H}^+} m_w c_{w,i} R^* T K_{\text{NH}_3}}{\gamma_{i,\text{NH}_4^+}}, \quad (5)$$

respectively. In Eqs. (4) and (5), the K's are equilibrium coefficients of the reactions, $HCl(g) \Leftrightarrow H^+ + Cl^-$ and $NH_3(g) + H^+ \Leftrightarrow NH_4^+$, respectively. In Eq. (4), γ is an activity coefficient of an electrolyte pair in a

mixture containing many electrolyte pairs. In Eq. (5)

$$\frac{\gamma_{i,\mathrm{H}^+}}{\gamma_{i,\mathrm{NH}_4^+}} = \frac{\gamma^2_{i,\mathrm{H}^+/\mathrm{NO}_3^-}}{\gamma^2_{i,\mathrm{NH}_4^+/\mathrm{NO}_3^-}} = \frac{\gamma^2_{i,\mathrm{H}^+/\mathrm{Cl}^-}}{\gamma^2_{i,\mathrm{NH}_4^+/\mathrm{Cl}^-}}. \quad (6)$$

A derivation of Eqs. (4) and (5) is given in Jacobson (1997b). Nitric acid (HNO_3) dissolution can be treated in a manner analogous to that of HCl dissolution. In Eqs. (3)–(5), $\mathbf{m}_{\mathrm{H}^+,i}$, $\gamma_{i,+/-}$, and $(dc_{q,i}/dt)_{\mathrm{eq}}$ must be obtained with a chemical equilibrium solver. The solver used here is EQUISOLV (Jacobson et al., 1996).

To conserve mass between the gas phase and all size bins of the particle phase, the gas-conservation equations,

$$\frac{dC_q}{dt} = -\sum_{i=1}^{N_B}\left[k_{q,i}(C_q - S'_{q,i}C_{q,s,i})\right], \quad (7)$$

$$\frac{dC_q}{dt} = -\sum_{i=1}^{N_B}\left[k_{q,i}\left(C_q - S'_{q,i}\frac{c_{q,i}}{H'_{q,i}}\right)\right] \quad (8)$$

are written for Eqs. (1) and (3), respectively, where, N_B is the number of particle size bins.

SOLUTION TO DISSOLUTIONAL GROWTH

Equations (3) and (8) represent $N_B + 1$ equations that must be solved simultaneously during dissolutional growth calculations. The scheme presented here, is called the *analytical predictor of dissolution* (APD) scheme. It requires no iteration, conserves mass exactly, and is unconditionally stable.

The solution to the dissolutional growth equations is obtained by first assuming that the final concentration of component q in size bin i is calculated by integrating Eq. (3). The resulting expression is

$$c_{q,i,t} = \frac{H'_{q,i,t-1}C_{q,t}}{S'_{q,i,t-1}} + \left(c_{q,i,t-1} - \frac{H'_{q,i,t-1}C_{q,t}}{S'_{q,i,t-1}}\right) \times \exp\left[-\frac{hS'_{q,i,t-1}k_{q,i,t-1}}{H'_{q,i,t-1}}\right] \quad (9)$$

where the subscripts t and $t-1$ indicate the current time and one time step backward, respectively, and h is the time step size(s). This equation relies on a final concentration, $C_{q,t}$, which is currently unknown. All final aerosol and gas concentrations are constrained by the mass-balance equation,

$$C_{q,t} + \sum_{i=1}^{N_B}(c_{q,i,t}) = C_{q,t-1} + \sum_{i=1}^{N_B}(c_{q,i,t-1}) = C_{\mathrm{tot}}. \quad (10)$$

Substituting Eq. (9) into Eq. (10) and solving for $C_{q,t}$ gives

$$C_{q,t} = \frac{C_{q,t-1} + \sum_{i=1}^{N_B}\left\{c_{q,i,t-1} \times \left(1 - \exp\left[-\frac{hS'_{q,i,t-1}k_{q,i,t-1}}{H'_{q,i,t-1}}\right]\right)\right\}}{1 + \sum_{i=1}^{N_B}\left\{\frac{H'_{q,i,t-1}}{S'_{q,i,t-1}} \times \left(1 - \exp\left[-\frac{hS'_{q,i,t-1}k_{q,i,t-1}}{H'_{q,i,t-1}}\right]\right)\right\}}, \quad (11)$$

which is the final gas concentration. This concentration is substituted into Eq. (9) to determine final aerosol concentrations.

Observation of Eqs. (11) and (9) indicate that neither can result in a negative concentration or a concentration greater than C_{tot}. Also, since Eq. (11) is derived from Eq. (10) and Eq. (10) is substituted into Eq. (9), $C_{q,t} + \Sigma_i c_{q,i,t}$ must always equal C_{tot}. Unconditional stability occurs when the absolute-value difference between a numerical and exact solution is bounded for all time, regardless of the time step (Celia and Gray, 1992). Because solutions from Eqs.

(9) and (11) are bounded between zero and C_{tot}, regardless of the time step, the APD scheme is unconditionally stable. To demonstrate, assume a gas dissolves in three particle size bins, where $k_{q,i,t-1} = 0.00333$, 0.00833, and 0.0117 s^{-1}, for the respective bins. Also, $H'_{i,q} = 4.0$, $S'_{q,i,t-1} = 1.0$, and $c_{q,i,t-1} = 0$ $\mu g\ m^{-3}$ for all bins and $C_{q,t-1} = 10$ $\mu g\ m^{-3}$. After two hours, the APD scheme predicted $C_{q,t} = 0.769$, $c_{q,1,t} = 3.08$, $c_{q,2,t} = 3.08$, and $c_{q,3,t} = 3.08$ $\mu g\ m^{-3}$, regardless of whether the time step was 0.1, 10, 60, 600, or 7200 s. In sum, the APD scheme conserves mass and is unconditionally stable.

SOLUTION TO CONDENSATIONAL GROWTH

Equations (1) and (7), together, represent $N_B + 1$ ordinary differential equations when the $(dc_{q,i}/dt)_{\text{eq}}$ terms are split out. The method presented to solve these equations is called the *analytical predictor of condensation* (APC) scheme. The scheme does not require iteration, conserves mass exactly, and is unconditionally stable.

The APC solution is obtained by assuming that the final concentration of component q in size bin i can be integrated from Eq. (1). A resulting implicit expression is

$$c_{q,i,t} = c_{q,i,t-1} + hk_{q,i,t-1}(C_{q,t} - S'_{q,i,t-1}C_{q,s,i,t-1}), \quad \textbf{(12)}$$

where $C_{q,t}$ is currently unknown. All final aerosol and gas concentrations are constrained by Eq. (10). Substituting Eq. (12) and Eq. (10) and solving for $C_{q,t}$ gives

$$C_{q,t} = \frac{C_{q,t-1} + h\sum_{i=1}^{N_B}\{k_{q,i,t-1}S'_{q,i,t-1}C_{q,s,i,t-1}\}}{1 + h\sum_{i=1}^{N_B}(k_{q,i,t-1})}. \quad \textbf{(13)}$$

The concentration from Eq. (13) cannot fall below zero but can increase above the total available mass of the species in the system. In such cases, gas concentration is limited by $C_{q,t} = \min[C_{q,t}, C_{\text{tot}}]$. This value now serves as an estimate and is substituted into Eq. (12). Equation (12) is limited by $c_{q,i,t} = \max[c_{q,i,t}, 0]$ to prevent evaporation beyond the total mass existing in each size bin. To ensure mass conservation when the latter limits are used, the final gas concentration is calculated as

$$C_{q,t} = C_{\text{tot}} - \sum_{i=1}^{N_B} c_{q,i,t}. \quad \textbf{(14)}$$

As with the APD scheme, the APC scheme is unconditionally stable. $C_{q,t}$ and $c_{q,i,t}$ are always bounded by 0 and C_{tot}, and $C_{q,t} + \Sigma_i c_{q,i,t}$ always equals C_{tot}. To demonstrate, assume a gas transfers between and among three particle size bins, where $k_{q,i,t-1} = 0.00833$, 0.001667, and 0.00667 s^{-1}, for the respective bins, $S'_{q,i,t-1} = 1.0$ for all three bins, $c_{q,i,t-1} = 2$, 5, and 0 $\mu g\ m^{-3}$ for the respective bins, $C_{q,t-1} = 3$ $\mu g\ m^{-3}$, and $C_{q,s,i,t-1} = 1$ $\mu g\ m^{-3}$. After four hours, the APC scheme predicted $C_{q,t} = 1.0$, $c_{q,1,t} = 2.18$, $c_{q,2,t} = 5.36$, and $c_{q,3,t} = 1.46$ $\mu g\ m^{-3}$, regardless of whether the time step was 0.1, 10, 60, 600, or 7200 s. Thus, the APC scheme conserves mass and is unconditionally stable.

SIMULATIONS UNDER ATMOSPHERIC CONDITIONS

Here, simulation results of condensation and dissolution coupled to equilibrium are shown for three cases representing typical conditions in coastal urban air. In all cases, the initial particle size distribution and composition contained four modes—one nucleation, two subaccumulation, and one coarse particle mode. The particles were assumed initially to contain only sulfuric acid, sodium chloride, elemental carbon, and nonreacting organic carbon. Sixteen size bins were used. The diameter of the smallest bin was 0.02 μm, and the volume ratio of adjacent size bins was 5.0. Figure 1 shows the initial distribution of water and ionic components in the particles when the relative humidity (r.h.) was 90% and the temperature was 298 K. The size bin struc-

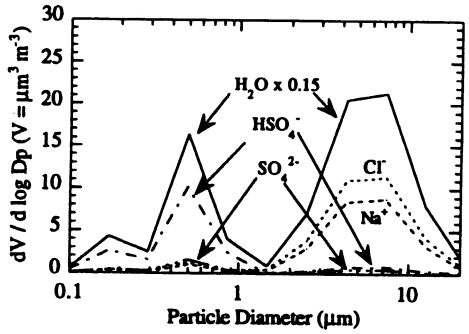

FIGURE 1. Initial model size distribution for r.h. = 90% and T = 298 K.

ture used was the *full-moving* structure (e.g., Jacobson, 1997a). With this structure, particles in each size bin grow and evaporate to their exact sizes.

For the first case, dissolutional growth was coupled to equilibrium at r.h. = 90%, over a four-hour simulation period. The dissolving species were HNO_3, NH_3, and HCl. After each time interval of growth, equilibrium was recalculated in each size bin, affecting the initial aqueous molality for the next dissolution calculation. Figure 2 shows a comparison of results from the APD/EQUISOLV scheme to those from the SMVGEAR II/EQUISOLV scheme when the time interval between growth and equilibrium was 1 s in both cases. Figure 2 also shows that the growth/equilibrium solutions nearly matched a pure equilibrium solution after about two hours, indicating that gas and aerosol phases were almost in equilibrium when the relative humidity was high. Figure 3 shows a case where the time interval between growth and equilibrium calculations was increased to 15 s. A time interval of 30 s (not shown) produced smooth, but slightly less accurate results. A time interval of 60 s (not shown) produced oscillations in sulfate and bisulfate concentrations caused by delays in feedback between dissociation reactions and growth calculations.

For the second case, dissolutional growth was coupled to equilibrium at r.h. = 40%. All other conditions were the same as those for the first simulation. Figure 4 shows a comparison of APD/EQUISOLV to SMVGEAR II/EQUISOLV solutions when the time interval between growth and equilibrium calculations was 10 s. The two solutions matched almost exactly. Figure 4 also shows that growth/equilibrium results converged to pure equilibrium results. In this case, convergence took more than 10 days. In the atmosphere, perturbations, such as emissions, chemistry, and transport affect gas and aerosol concentrations over

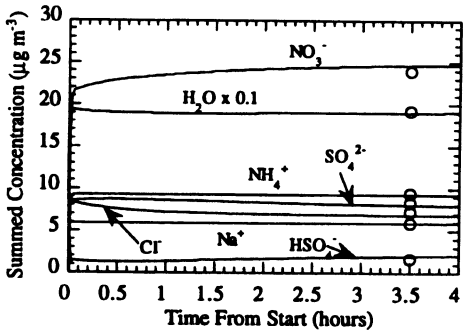

FIGURE 2. Time-series comparison of APD/EQUISOLV results to SMVGEAR II/EQUISOLV results when a 1 s interval was used between growth and equilibrium. The solutions from both methods lie almost exactly on top of each other. Also shown are equilibrium solution (circles), calculated from EQUISOLV alone. Initial conditions were r.h. = 90%, T = 298 K, $HNO_3(g) = 30$, $NH_3(g) = 10$, and $HCl(g) = 0$ $\mu g\ m^{-3}$.

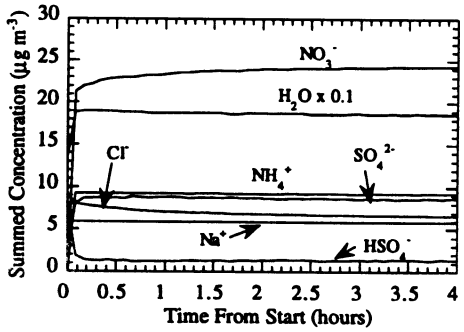

FIGURE 3. Time-series plot of APD/EQUISOLV results when the time interval between growth and equilibrium was 15 s. Compare to Fig. 2.

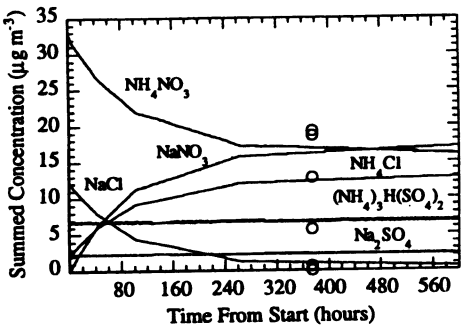

FIGURE 4. Time-series comparison of APD/EQUISOLV results to SMVGEAR II/EQUISOLV results when a 10 s interval was used between growth and equilibrium. The solutions from both methods lie almost exactly on top of each other. The figure also shows equilibrium solutions (circles), calculated from EQUISOLV alone. Circle values are $Na_2SO_4 = 0.583$; NaCl = 0.596; $NaNO_3 = 18.6$; $(NH_4)_2SO_4 = 0$; $NH_4Cl = 12.8$; $NH_4NO_3 = 19.2$; and $(NH_4)_3H(SO_4)_2 = 5.68$ $\mu g\ m^{-3}$. Initial conditions were r.h. = 40%, T = 298 K, $HNO_3(g) = 30$, $NH_3(g) = 10$, and HCl(g) = 0 $\mu g\ m^{-3}$.

much shorter time periods. Thus, when the relative humidity is low, gases may not reach equilibrium with aerosols. Figure 5 shows the APD/EQUISOLV solution when the interval between growth and equilibrium calculations was 15 s. A time interval of 60 s (not shown) produced oscillations in concentrations of several species.

For the third case, cloud drop formation and with gas absorption were simulated. Growth processes accounted for included dissolution of $HNO_3(g)$, $NH_3(g)$, and HCl(g) and condensation of $H_2SO_4(g)$ and $H_2O(g)$. Conditions for the simulation are described in the caption for Fig. 6. The figure shows a time-series comparison of the APD/APC/EQUISOLV solution to the SMVGEAR II/EQUISOLV solution when the time interval between growth and equilibrium was 10 s. The solutions from the two schemes matched exactly for almost all species. Figure 7 shows the size distribution of liquid water initially, after growth, and after evaporation, for the simulations shown in Fig. 6. In the case of cloud drop growth, a longer time interval of 60 s (not shown) between growth and equilibrium calculations did not produce oscillations in concentrations because dilute solutions mollified the feedback of dissociation reactions on growth calculations.

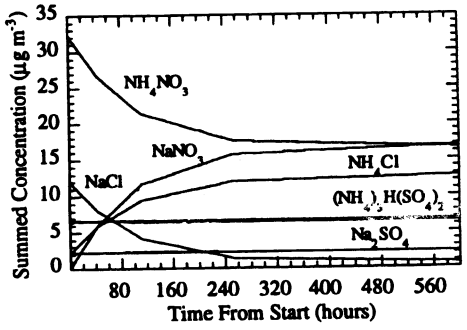

FIGURE 5. Time-series plot of APD/EQUISOLV results when the time interval between growth and equilibrium was 15 s. Compare to Fig. 4.

COMPUTER TIMINGS

Computer timing tests were performed for the cases shown in Figs. 3 and 5. Simulation times shown are for growth and equilibrium

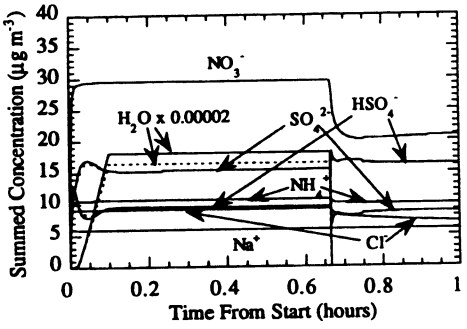

FIGURE 6. Time-series comparisons of APD/APC/EQUISOLV results to SMVGEAR II/EQUISOLV results when a 10 s interval was used between growth and equilibrium for both schemes. The two solutions lie almost exactly on top of one another for all species except liquid water. Initial conditions were T = 298 K, $HNO_3(g) = 30$, $NH_3(g) = 10$, HCl(g) = 0, and $H_2SO_4(g) = 15$ $\mu g\ m^{-3}$. At time zero, the r.h. was increased from 90% to 100.001%. The r.h. was then reset to 100.001% after every 10 s growth calculation for the first five minutes. After forty minutes, the r.h. was reduced to 90%.

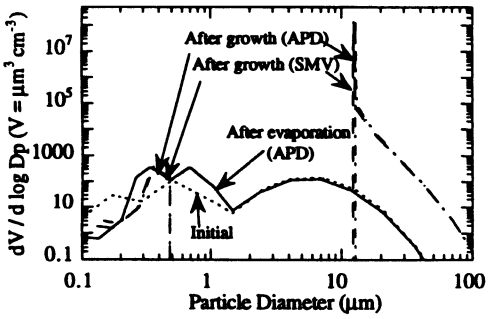

FIGURE 7. Model size distribution initially, after growth, and after evaporation obtained from the simulation shown in Fig. 6. Growth solutions for both APD / APC / EQUISOLV (APD) and SMVGEAR / EQUISOLV (SMV) are shown.

calculations, together. Equilibrium calculations took more than 90% of the total time in both cases. Test were performed on the Cray J-916, a vector processing machine with a speed approximately one-fifth the speed of a Cray 90. The simulation shown in Fig. 3 required 0.179 s per grid cell per hour of simulation on the Cray J-916. For a 20,000-cell grid, this translates to about 23.9 hours per day on the Cray J-916 and 4.78 hours per day on the Cray 90. The simulation shown in Fig. 5 required 1.19 s per grid cell per hour of simulation. For a 20,000-cell grid, this translates to about 160 hours per day on the Cray J-916 and 31.9 hours per day on the Cray 90. The solution time for the low relative humidity case was greater than that for the high humidity case because more equilibrium equations were solved in the former case. The computer times of the APC and APD schemes, which are noniterative, were approximately one-half those of SMVGEAR II, which is iterative. Because the matrix of partial derivatives in SMVGEAR II was sparse and required no fill-in, SMVGEAR II speeds were fast for this application.

CONCLUSIONS

Noniterative, unconditionally stable, mass-conserving numerical schemes were developed to solve growth equations. The analytical predictor of condensation (APC) scheme solves condensational growth equations, and the analytical predictor of dissolution (APD) scheme solves dissolutional growth equations. Results from the APD and APC schemes were compared to Gear-code (SMVGEAR II) results when growth was coupled to an equilibrium solver (EQUISOLV). In the three cases tested, APD/APC/EQUISOLV solutions matched SMVGEAR II/EQUISOLV solutions when the time interval between growth and equilibrium was 1 s. Solutions were also good when the time interval between growth and equilibrium was 15 s. When the latter time interval is used, the coupled equilibrium/growth schemes can be used in three-dimensions. Simulation results indicated that, at a high relative humidity, growth/equilibrium approached pure equilibrium after about two hours. At a low relative humidity, equilibrium was reached after more than ten days.

This work was funded by grants from the Environmental Protection Agency under assistance agreement 823186-01-0, the Charles Lee Powell Foundation, and the National Science Foundation under agreement ATM-9504481.

References

Bott, A., and Carmichael, G. R. (1993). Multiphase Chemistry in a Microphysical Radiation Fog Model—A Numerical Study, *Atmos. Environ.* 27A:503–522.

Brock, J. R., Zehavi, D., and Kuhn, P. (1986). Condensation Aerosol Formations and Growth in a Laminar Coaxial Jet: Experimental, *J. Aerosol Sci.* 17:11–22.

Celia, M. A., and Gray, W. G. (1992). *Numerical Methods for Differential Equations*. Prentice Hall, Englewood Cliffs, NJ, 436 pp.

Chameides, W. L. (1984). The Photochemistry of a Remote Marine Stratiform Cloud, *J. Geophys. Res.* 89:4739–4755.

Friedlander, S. K. (1983). Dynamics of Aerosol Formation by Chemical Reaction, *Ann. NY Acad. Sci.* 404:354–364.

Gelbard, F., and Seinfeld, J. H. (1980). The General Dynamic Equation for Aerosols:

Theory and Application to Aerosol Formation and Growth, *J. Colloid Interface Sci.* 78:485–501.

Jacob, D. (1986). Chemistry of OH in Remote Clouds and its Role in the Production of Formic Acid and Peroxymonosulfate, *J. Geophys. Res.* 91:9807–9826.

Jacobson, M. Z., and Turco, R. P. (1995). Simulating Condensational Growth, Evaporation, and Coagulation of Aerosols Using a Combined Moving and Stationary Size Grid, *Aerosol Sci. and Technol.* 22:73–92.

Jacobson, M. Z., Tabazadeh, A., and Turco, R. P. (1996). Simulating Equilibrium Within Aerosols and Nonequilibrium Between Gases and Aerosols, *J. Geophys. Res.* 101:9079–9091.

Jacobson, M. Z. (1997a). Development and Application of a New Air Pollution Modeling System—II: Aerosol Module Structure and Design, *Atmos. Environ.* 31A:131–144.

Jacobson, M. Z. (1997b). *Fundamentals of Atmospheric Modeling.* Cambridge University Press (in publication).

Lee, K. W. (1985). Conservation of Particle Size Distribution Parameters during Brownian Coagulation, *J. Colloid and Interface Sci.* 108:199–206.

Middleton, P. and Brock, J. R. (1976). Simulation of Aerosol Kinetics. *J. Colloid Interface Sci.* 54:249–264.

Pandis, S. N. and Seinfeld, J. H. (1989). Sensitivity Analysis of a Chemical Mechanism for Aqueous-phase Atmospheric Chemistry. *J. Geophys. Res.* 94:1105–1126.

Rao, N. P. and McMurry, P. H. (1989). Nucleation and Growth of Aerosol in Chemically Reacting Systems: A Theoretical Study of the Near-collision-controlled Regime. *Aerosol Sci. Technol.* 11:120–133.

Sander, R., Lelieveld, J. and Crutzen, P. J. (1995). Modelling of the Nighttime Nitrogen and Sulfur Chemistry in Size Resolved Droplets of an Orographic Cloud, *J. Atmos. Chem.* 20: 89–116.

Schwartz, S. E., (1984). Gas- and Aqueous-phase Chemistry of HO_2 in Liquid-Water Clouds, *J. Geophys. Res.* 89:11,589–11,598.

Smolarkiewicz, P. K. (1983). A Simple Positive Definite Advection Scheme with Small Implicit Diffusion, *Mon. Weather Rev.* 111:479–486.

Toon, O. B., Turco, R. P., Westphal, D., Malone, R., and Liu, M. S. (1988). A Multidimensional Model for Aerosols: Description of Computational Analogs, *J. Atmos. Sci.* 45: 2123–2143.

Tsang, T. H., and Brock, J. R. (1986). Simulation of Condensation Aerosol Growth by Condensation and Evaporation, *Aerosol Sci. Technol.* 5:385–388.

Tsang, T. H., and Huang, L. K. (1990). On a Petrov–Galerkin Finite Element Method for Evaporation of Polydisperse Aerosols, *Aerosol Sci. Technol.* 12:578–597.

Tsang, T. H., and Korgaonkar, N. (1987). Effect of Evaporation on the Extinction Coefficient of an Aerosol Cloud, *Aerosol Sci. Technol.* 7:317–328.

Varoglu, E., and Finn, W. D. L. (1980). Finite Elements Incorporating Characteristics for One-dimensional Diffusion-convection Equation, *J. Comp. Phys.* 34:371–389.

Wexler, A. S., and Seinfeld, J. H. (1991). Second-generation Inorganic Aerosol Model, *Atmos. Environ.* 25A:2731–2748.

Whitby, E. R. (1985). *The Model Aerosol Dynamics Model. Part I.* Report to the U.S. Environmental Protection Agency, Dept. of Mechanical Engineering, University of Minnesota, Minneapolis.

Received February 9, 1996; accepted June 4, 1997.